



*Research article*

## **Discontinuous maneuver trajectory prediction based on HOA-GRU method for the UAVs**

**Zhizhou Zhang<sup>1</sup>, Zhenglei Wei<sup>2,\*</sup>, Bowen Nie<sup>2</sup> and Yang Li<sup>1</sup>**

<sup>1</sup> School of Aeronautics and Astronautics, Sun Yat-sen University, Guangzhou 510275, China

<sup>2</sup> Low Speed Aerodynamics Institute, China Aerodynamics Research and Development Center, Mianyang 621000, China

\* **Correspondence:** Email: zhenglei\_wei@126.com.

**Abstract:** With the rapid development of artificial intelligence technology, the intelligence and autonomy of Unmanned Aerial Vehicles (UAVs) have been significantly improved. Because the real trajectory data is often discontinuous and random, the current aircraft maneuver trajectory prediction methods are far from meeting the practical requirements of the autonomous air tasks. Especially, in order to occupy a better position rapidly where it is easier to attack the enemy, a fast and accurate maneuver trajectory prediction method for the UAVs is proposed in this paper. Firstly, the prediction model of aircraft maneuvering trajectory is built by extracting characteristic information from the historical trajectory. Aiming at the problem of slow optimization speed and easy to fall into local optimization, a global aircraft maneuver trajectory prediction method based on the Hummingbird Optimization Algorithm (HOA) and Gated Recurrent Unit (GRU) is proposed. Then, the implementation process of the maneuver trajectory prediction method based on the above HOA-GRU network for the UAVs is presented. Finally, the aircraft maneuver trajectory prediction method is applied to a simulation training system with the discontinuous and random air task data. The simulation results show that the proposed method can predict the maneuver trajectory of the UAVs with discontinuous data in real time with less error and less time.

**Keywords:** Unmanned Aerial Vehicle; aircraft maneuver trajectory prediction; Hummingbird Optimization Algorithm; Gated Recurrent Unit; discontinuous data; differential dynamical system

---

## 1. Introduction

The Unmanned Aerial Vehicles (UAVs) can complete a variety of complex air tasks, and are playing a more and more important role in the mordent wars. Because there is no need to consider the limitations of human physical conditions, the UAVs can give full play to the performance of aircraft and make large overload maneuvers that are difficult for manned aircraft. Especially, with the rapid development of artificial intelligence technology, the degree of intelligence and autonomy of the UAVs has been improved quickly. The intelligence of the UAVs in the autonomous air tasks integrates the detection, predictive identification, tracking, decision-making, control functions, and so on [1]. It should be pointed out that, as an important link in the autonomous air tasks of the UAVs, the aircraft trajectory prediction strategy can provide the future aircraft flight trajectory in advance, and shorten the time needed for task decision, and occupy the better positions where it is easier to attack the enemies [2]. Therefore, in order to occupy better attack positions, it is necessary to study the fast and accurate maneuver trajectory prediction technology for the UAVs.

Because the air task is very fierce and changeable, the trajectory prediction model of the UAVs is highly nonlinear and time-varying [2]. With the nonlinear and time-variable historical trajectory information and complex situation information, it is difficult to predict the future trajectory characteristic information rapidly and accurately for the UAVs [3]. So far, there are many research results on the trajectory prediction methods of the UAVs. Generally speaking, they can be divided into two categories: one is model-driven, the other is data-driven.

The model-driven trajectory prediction method needs to acquire the prior knowledge and the motion law of the aircraft at first, and then constructs a very accurate dynamic or kinematic model [4]. Reference [5] proposes a Bayes trajectory prediction method based on intention speculation. Reference [6] gives a trajectory prediction method, which is realized by linear fitting of lift-drag ratio state function combined with numerical integration. Reference [7] presents a trajectory prediction method based on grey dynamic filtering. Reference [8] uses an extended Kalman filter to estimate the motion state of the UAVs, and then calculates the trajectory combined with the motion model. For the model-driven methods above, they are extremely sensitive to the initial states and model parameters of the aircraft. Only when the initial state value is of high accuracy and the model parameters can be accurately estimated, the result of the aircraft trajectory prediction may be more accurate [9,10].

The data-driven method is to analyze the historical trajectory data of the aircraft, and mine the flight rules hidden in the data, so as to realize the prediction of the spatial position of the aircraft in the future time. A BP neural network is used to construct the trajectory prediction system, which realizes the accurate prediction of the flight trajectory in a short time [11]. Reference [12] uses an improved particle swarm optimization algorithm to optimize the trajectory prediction method based on Elman neural network. Reference [13] proposes a trajectory prediction method based on winding neural network, which improved the prediction accuracy of complex trajectory greatly. Reference [14] uses the Gated Recurrent Unit (GRU) to predict the flight trajectory, which has a smaller prediction error than the BP network. Thus, the data-driven trajectory prediction methods above do not need to establish an accurate motion model of the aircraft in advance, and the prediction system is simple and real-time. However, the data-driven trajectory prediction methods have more requirements of the rationality of the data itself, and the adjustment of system parameters may be time-consuming.

In order to avoid dependence on accurate models and reasonable data and improve prediction accuracy and prediction speed, this paper proposes an aircraft maneuver trajectory prediction method.

The contributions of this paper are summarized in the following two aspects.

- 1) An aircraft maneuver trajectory prediction method based on the Hummingbird Optimization Algorithm (HOA) to optimize the GRU prediction network is proposed. This method avoids the disadvantages of traditional GRU network for the UAVs, such as slow optimization speed and easy to fall into local optimization.
- 2) The maneuver trajectory prediction method based on HOA-GRU for the UAVs is presented. This method combines the advantages of model-driven method and data-driven method, and obtains a better prediction accuracy and speed for the UAVs.

The remainder of this paper is organized as follows. In Section 2, the historical trajectory characteristics of aircraft are extracted and the prediction model of aircraft maneuver trajectory is built. In Section 3, in order to avoid the slow optimization speed and local optimization of the previous prediction methods, the HOA is used to optimize the GRU prediction network, and then a global optimal maneuver trajectory prediction method based on HOA-GRU is proposed. In Section 4, the flow and steps of maneuver trajectory prediction method based on HOA-GRU for the UAVs are presented. In Section 5, the HOA-GRU prediction method is applied to a simulation system with lots of real flight data. Finally, the effectiveness of the proposed trajectory prediction method is verified by some simulation experiments.

## 2. Maneuver trajectory prediction modeling of the UAVs

For the convenience of analysis, the maneuvering trajectory model of the UAVs needs to be established in this section.

It is assumed that the airborne radar of the UAV can obtain the historical trajectory information of the other side's aircraft, including the specific position  $P_{e,t-1} = [x_{e,t-1}, y_{e,t-1}, z_{e,t-1}]$  at time  $t-1$  and  $P_{e,t} = [x_{e,t}, y_{e,t}, z_{e,t}]$  at the time  $t$  in the X-Y-Z coordinate system. If the time interval of the time  $t-1$  and  $t$  is  $\Delta t$ , the velocity of the aircraft is:

$$v_{e,t} = \frac{(P_{e,t} - P_{e,t-1})}{\Delta t} \quad (1)$$

Then the velocity change rate of the aircraft is:

$$\Delta v_{e,t} = \frac{(v_{e,t} - v_{e,t-1})}{\Delta t} \quad (2)$$

The change rate of the deviation angle of the trajectory,  $\Delta\psi_{e,t}$ , which denotes the intersection angle between the due east direction and the projection of the instantaneous motion direction of the aircraft onto the ground plane, can be obtained as:

$$\Delta\psi_{e,t} = \begin{cases} \arctan\left(\frac{(x_{e,t} - x_{e,t-1})}{(y_{e,t} - y_{e,t-1})}\right), & x_{e,t} - x_{e,t-1} \geq 0 \\ \pi + \arctan\left(\frac{(x_{e,t} - x_{e,t-1})}{(y_{e,t} - y_{e,t-1})}\right), & x_{e,t} - x_{e,t-1} < 0, y_{e,t} - y_{e,t-1} \geq 0 \\ -\pi - \arctan\left(\frac{(x_{e,t} - x_{e,t-1})}{(y_{e,t} - y_{e,t-1})}\right), & x_{e,t} - x_{e,t-1} < 0, y_{e,t} - y_{e,t-1} < 0 \end{cases} \quad (3)$$

Here, the altitude of the aircraft at time  $\mathbf{t}$  of the aircraft,  $H_{e,t}$ , can be acquired by our airborne radar. Then the change in altitude of an aircraft is  $\Delta H_{e,t} = \frac{(H_{e,t} - \Delta H_{e,t-1})}{\Delta t}$ .

The change rate of inclination angle of the trajectory,  $\Delta\theta_{e,t}$ , which denotes the angle between the horizontal plane and the instantaneous motion direction of the aircraft, can be expressed as:

$$\Delta\theta_{e,t} = \arctan\left(\frac{\Delta H_{e,t}}{\sqrt{(x_{e,t} - x_{e,t-1})^2 + (y_{e,t} - y_{e,t-1})^2}}\right) \quad (4)$$

From Eqs (1)–(4), we can get the characteristics of the maneuver trajectory of the aircraft  $X_e = [\Delta\psi_e, \Delta\theta_e, \Delta H_e, \Delta v_e]$  of the aircraft. Here,  $\Delta\psi_e$  is the rate of change in the deflection angle,  $\Delta\theta_e$  is the rate of change in the inclination angle,  $\Delta H_{e,t}$  is the rate of change in the altitude of the aircraft,  $\Delta v_e$  is the rate of change in the speed of the aircraft.

Assume that  $X_e = [\Delta\psi_e, \Delta\theta_e, \Delta H_e, \Delta v_e]$  is the characteristic parameters of the historical trajectory of the aircraft, and  $Y_e = [\Delta\psi_e, \Delta\theta_e, \Delta H_e, \Delta v_e]$  is the characteristic parameters of the future trajectory of the aircraft. Based on the historical data  $X_e$  from the airborne radar, the future data  $Y_e$  is expected to be predicted. This is a prediction problem of the trajectory of the aircraft.

Based on the actual flight data, we can get a set of the training samples  $S = \{(X_e, Y_e) | X_e = X_{e,i}, Y_e = X_{e,j}\}$ , where  $i = t - n + 1 : t, j = t + 1 : t + m, n > 0, m > 0$ . Now, the problem of maneuver trajectory prediction of the aircraft can be defined as:

$$Y_{e,j} = f_{pred}(X_{e,i} | S) = f_{pred}(X_{e,i} | \theta_{pred}) \quad (5)$$

where,  $X_{e,i}$  is the input variable for past time  $i$ ,  $Y_{e,j}$  is the predicted output variable at the future time  $j$ ,  $f_{pred}$  is the prediction algorithm of the future trajectory of the aircraft,  $\theta_{pred}$  is the parameters of the predict network.

According to Eq (5), assuming that the current time is  $\mathbf{t}$  and the prediction time interval is  $\Delta t$ , the future trajectory of the aircraft at the next time  $\mathbf{t}+1$  can be calculated as follows:

$$\psi_{e,t+1} = \psi_{e,t} + \Delta\psi_{e,t+1} \cdot \Delta t \quad (6)$$

$$\theta_{e,t+1} = \theta_{e,t} + \Delta\theta_{e,t+1} \cdot \Delta t \quad (7)$$

$$v_{e,t+1} = v_{e,t} + \Delta v_{e,t+1} \cdot \Delta t \quad (8)$$

$$\begin{bmatrix} x_{e,t+1} \\ y_{e,t+1} \\ z_{e,t+1} \end{bmatrix} = \begin{bmatrix} x_{e,t} \\ y_{e,t} \\ z_{e,t} \end{bmatrix} + \begin{bmatrix} v_{e,t+1} \cos \theta_{e,t+1} \cos \psi_{e,t+1} \\ v_{e,t+1} \cos \theta_{e,t+1} \sin \psi_{e,t+1} \\ \Delta H_{e,t+1} \cdot \Delta t \end{bmatrix} \quad (9)$$

where  $x_{e,t+1}$ ,  $y_{e,t+1}$ ,  $z_{e,t+1}$ ,  $\theta_{e,t+1}$ ,  $\psi_{e,t+1}$  and  $v_{e,t+1}$  are respectively represent the predicted position of the aircraft in the X-Y-Z coordinate system, the inclination angle of the trajectory, the deflection angle and the speed of the aircraft at time  $t + 1$ . Here,  $z_{e,t+1}$  is denoted by the height of the aircraft  $\Delta H_{e,t+1}$  in Eq (9).

### 3. Global optimal prediction method based on HOA-GRU algorithm

Based on the prediction model of the maneuver trajectory in Section 2, this section focuses on the effective global optimization strategy of the maneuver trajectory prediction of the UAVs.

Firstly, a GRU search strategy is proposed to overcome the problem of gradient disappearance for the long time series prediction. Then, in order to avoid the gradient optimization of GRU falling into local optimization, the depth optimization based on HOA is proposed. Finally, combining the advantages of the above GRU and HOA, a kind of HOA-GRU optimization algorithm is proposed to avoid the disadvantages of traditional GRU network for the UAVs, such as slow optimization speed and easy to fall into local optimization.

### 3.1. Long term optimization strategy based on GRU

Recurrent Neural Network (RNN) provides an effective solution to the problem of time series prediction [15], but there are some problems including the gradient explosion and gradient disappearance when dealing with long-term time series problems. As the advanced versions of RNN, the Long Short-term Memory (LSTM) [16] and GRU [17] strategy effectively solve the gradient problem of RNN. Compared with LSTM, GRU has a simpler structure and fewer parameters. By introducing the gate structure, the GRU is composed of update door and reset door for the UAVs. The schematic diagram of GRU network is shown in Figure 1.

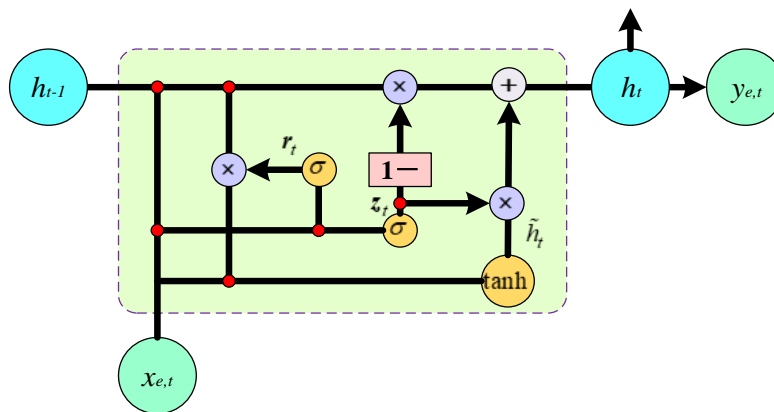


**Figure 1.** GRU network diagram.

The specific model structure of the GRU is as follows. The current information of the Candidate's hidden layer is given as:

$$r_t = \sigma(W_{hr}h_{t-1} + W_{xr}x_t + b_r) \quad (10)$$

$$\tilde{h}_t = \tanh(W_{rh}(r_t * h_{t-1}) + W_{xh}x_t + b_h) \quad (11)$$

where  $r_t$  is the reset of the door, which determines how much historical memory to retain.  $\tilde{h}_t$  is the latest information at the current time in the Candidate hidden layer,  $h_{t-1}$ ,  $h_t$  are respectively the information at the time t-1 and t in the Candidate hidden layer.  $W_{rh}$ ,  $W_{xh}$ ,  $W_{xr}$ ,  $W_{hr}$  are the weight coefficients,  $b_r$ ,  $b_h$  are the offset coefficients.  $\sigma$  is the specific coefficient.

$$z_t = \sigma(W_{hz}h_{t-1} + W_{xz}x_t + b_z) \quad (12)$$

$$h_t = (1 - z_t) * h_{t-1} + z_t * \tilde{h}_t \quad (13)$$

where,  $W_{hz}$ ,  $W_{xz}$  are the weight,  $b_z$  is the offset,  $z_t$  is the forgetting gate, which is used to record the hidden layer information input  $h_{t-1}$  at the last time and the current information  $\tilde{h}_t$ , and obtain the output information  $h_t$ . If  $z_t = 0$ , the hidden layer directly outputs the hidden layer information  $h_{t-1}$  of the previous time, and if  $z_t = 1$ , the candidate hidden layer directly outputs the information  $h_t$  of the current hidden layer:

$$y_t = \sigma(W_{yt}h_t) \quad (14)$$

where,  $W_{yt}$  represents weight between the current hidden layer output  $h_t$  and the final output layer.

### 3.2. Random optimization strategy based on HOA

HOA is a random optimization algorithm that simulates the process of hummingbird honey collection. At the beginning of the algorithm, multiple hummingbird individuals are randomly created in the search space [18]. The position of each individual corresponds to a feasible solution of the optimization problem. The quality of food source is the value of objective function, and the best food source is the global optimal solution. The whole process of HOA can be divided into two phases: the self-searching phase and the guided searching phase. The specific form of the algorithm is as follows:

#### 1) Self-searching phase

Assume that the population size of hummingbirds is  $NP$  and the dimension in the search space is  $D$ .  $X_i^t = \{x_{i,1}^t, x_{i,2}^t, x_{i,3}^t, \dots, x_{i,D}^t\}$  represents the  $i$ th hummingbird individual at time  $t$ . During the self-searching phase, hummingbirds can look for food sources based on their previous experience. When hummingbirds can constantly find better sources of food ( $X_i^t \neq X_i^{t-1}$ ), the validity of previous experience is verified. Therefore, the position of each hummingbird is updated based on the previous gradient information:

$$X_i^{t+1} = X_i^t + rand \cdot (X_i^t - X_i^{t-1}) \quad (15)$$

where,  $X_i^t$  and  $X_i^{t-1}$  respectively represent the position of the 3116th hummingbird at  $t$  and  $t - 1$ , and  $rand$  denotes the random number in the range  $[0, 1]$ .

When the hummingbird keeps searching and finds no better results ( $X_i^t \neq X_i^{t-1}$ ), it means that the hummingbird's past experience no longer applies. In this case, the hummingbird randomly changes its search direction. This process was simulated using a Levy flight. Levy flight is an important non-Gaussian random walk whose random step size follows a large-tailed probability distribution. The most important feature of this flight mode is that it maximizes space exploration in uncertain environments, because of the infinite and rapid growth of variance. A Levy flight can search more efficiently than a regular random walk such as the Brownian motion [19].

The Levy flight is capable of producing larger jumps than the Brownian motion, thus exploring space more widely. Therefore, it is more suitable for large-scale search. The search process based on Levy flight is expressed as follows:

$$X_i^{t+1} = X_i^t + \alpha_0(X_i^t - X_{best}^t) \oplus Levy(\beta) \quad (16)$$

Here,  $X_{best}^t$  represents the global optimal solution at the time  $t$ ,  $\alpha_0 = 0.01$  is the scale factor,

$\oplus$  is scalar-multiplication. Then,  $Levy(\beta)$  can be computed as:

$$Levy(\beta) = \frac{\mu}{|v|^{1/\beta}} \quad (17)$$

where  $\mu$  and  $v$  respectively represent two random numbers that follow the Gaussian distribution  $N(0, \sigma_\mu^2)$  and  $N(0, \sigma_v^2)$ , where

$$\sigma_\mu = \left( \frac{\Gamma(1+\beta) \sin(\pi\beta/2)}{\Gamma[(1+\beta)/2] \beta 2^{(\beta-1)/2}} \right)^{1/\beta}, \sigma_v = 1 \quad (18)$$

where  $\Gamma(z)$  represents the gamma function, and the size of  $\beta$  is set to 1.5 [19].

## 2) Guided-searching phase

At this stage, the current best hummingbird individuals are called territorial birds, and the other individuals are called follower birds. The territorial bird patrols its territory to keep other birds away. This behavior can be expressed as:

$$X^{T,t+1} = X^{T,t} + r_d \cdot \lambda \quad (19)$$

where  $X^{T,t}$  represents the position of the territorial bird at the moment  $t$ ,  $X^{T,t}$  is a random number in the range of  $[-1, 1]$ , and  $r_d$  is the specific coefficient.  $\lambda$  is the step factor, defined as follows:

$$\lambda = 0.1 \cdot (ub - lb) \quad (20)$$

where  $ub$  and  $lb$  respectively represent the upper and lower bounds of the search space.

There are two ways to follow a hummingbird [19].

**Case 1:** when the territorial bird finds no threat, the follower bird will approach the territory quickly:

$$X_j^{F,t+1} = X_j^{F,t} + rand \cdot (X^{T,t} - MF \cdot X_j^{F,t}) \quad (21)$$

where  $X_j^{F,t}$  is the position of the  $j$ -th follower bird at time  $T$ ,  $MF$  is a random value of 1 or 2.

**Case 2:** When the territorial bird finds the follower, the follower is driven away and flies around. During this process, the follower bird  $j$  will randomly select a companion  $k(k \neq j)$  to follow. If the position  $k$  is better, it will move toward it, otherwise, it will move away. The above can be expressed by the following formula:

$$X_j^{F,t+1} = X_j^{F,t} + rand \cdot (X_k^{F,t} - X_j^{F,t}), \text{ if } fitX_k^{F,t} \leq fitX_j^{F,t} \quad (22)$$

$$X_j^{F,t+1} = X_j^{F,t} - rand \cdot (X_k^{F,t} - X_j^{F,t}), \text{ if } fitX_k^{F,t} \geq fitX_j^{F,t} \quad (23)$$

where  $j, k \in \{1, 2, 3, \dots, N-1\}$ ,  $j \neq k$ ,  $fitX_k^{F,t}$  and  $fitX_j^{F,t}$  are respectively the fitness value of  $X_k^{F,t}$  and  $X_j^{F,t}$ .

To sum up, the complete search process of following birds is described as follows:

if  $PF^t \geq rand$   
 {to carry out the **Case 1**;}  
 else  
 {to carry out the **Case 2**.}

where the probability of the following bird being discovered by the territorial bird can be calculated by the formula:

$$PF^t = \frac{rank(fitX_j^{F,t})}{N-1} \quad (24)$$

where  $rank(fitX_j^{F,t})$  represents the rank of the following bird  $j$  among all companions according to fitness value.

In addition, the boundary control policy for preventing invalid searches can be described as follows:

$$X_{i,d}^t = ub - rand \cdot (ub - lb), \text{ if } X_{i,d}^t < lb \text{ or } X_{i,d}^t > ub \quad (25)$$

Finally, HOA adopts the greedy strategy to update the population. That is to say, only when the fitness value  $X_i^{t+1}$  of is better than  $X_i^t$ , the individual  $X_i^{t+1}$  will be retained; otherwise, the individual will not be updated. This scenario is described as follows:

$$X^{t+1} = \begin{cases} X^{t+1} & \text{if } f(X^{t+1}) < f(X^t) \\ X^t & \text{otherwise} \end{cases} \quad (26)$$

### 3.3. Global prediction method of GRU network optimized by HOA

As can be seen from the above analysis, the GRU has the advantages of simple structure and few parameters when predicting long time series, but the optimization speed is slow and it is easy to fall into local optimization. The HOA has strong global search ability and better adaptability. Therefore, an HOA-GRU optimization algorithm is proposed to effectively avoid the shortcomings of GRU network.

The whole idea of optimizing GRU network parameters based on HOA is to optimize the weight and bias parameters in the GRU network after training by using the strong global search ability, local exploration ability and high adaptability of HOA. The parameters are constantly adjusted according to the fitness function, and finally the best parameters of the GRU prediction network are obtained.

In the GRU network, there are 10 parameters that need to be optimized, and they are respectively  $W_{rh} \in I^{h*n}$ ,  $W_{xh} \in I^{h*h}$ ,  $W_{xr} \in I^{h*n}$ ,  $W_{hr} \in I^{h*h}$ ,  $W_{xz} \in I^{h*n}$ ,  $W_{hz} \in I^{h*h}$ ,  $W_{yt} \in I^{m*h}$ ,  $b_r \in I^{h*1}$ ,  $b_{\tilde{h}} \in I^{h*1}$ ,  $b_z \in I^{h*1}$ . Here,  $h$  is the number of hidden layers,  $n$  is the number of historical data, and  $m$  is the number of steps to predict the future. The HOA needs to optimize all parameters in the GRU network, and the search dimension  $D$  is  $3 * (h * n) + 3(h * h) + 3 * (h * 1) + m * h$ .

In the training process of HOA, the fitness function is required to guide the optimization direction of the algorithm, update the population and gradient, and solve the minimum fitness value until the termination condition of the algorithm is met. Therefore, the fitness function is:

$$fitness = \sum_{i=1}^{n_e} (Y_{e,i} - f_{pred}(X_{e,i} | \theta_{pred}))^2 \quad (27)$$



where  $n_e$  is the time sequence length of the training data,  $Y_{e,i}$  is the actual output value,  $f_{pred}(X_{e,i}|\theta_{pred})$  is the output value of the prediction model, and  $\theta_{pred}$  is the GRU optimization parameter.

#### 4. Procedure of aircraft maneuver trajectory prediction method based on HOA-GRU network

Combining atomic search optimization algorithm and GRU network, this section proposes an aircraft maneuver trajectory prediction method based on HOA optimized GRU network. The prediction model mainly takes the characteristic time series of the maneuver trajectory at the historical moment as the input and the characteristic time series of the maneuver trajectory at the future moment as the output, to dig the motion law of the maneuver trajectory.

The maneuver trajectory prediction process based on HOA-GRU is shown in Figure 2.

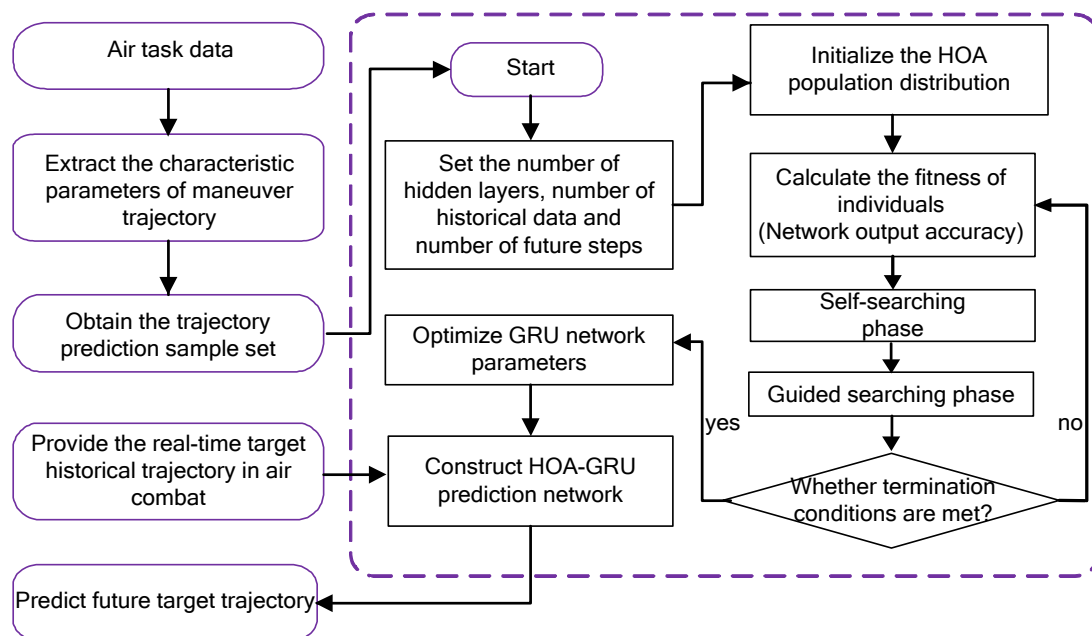


**Figure 2.** Flow chart of target maneuver trajectory prediction.

The specific steps are as follows:

**Step 1:** The prediction sample set of aircraft maneuver trajectory is constructed by extracting the characteristic parameters of air confrontation data maneuver trajectory;

**Step 2:** Determine the GRU network structure, and take the bias value and weight value as the optimization object of HOA;

**Step 3:** Initialize the atomic population distribution of HOA according to the GRU network structure;

**Step 4:** According to Eq (27), the fitness value of individual hummingbirds of HOA is calculated to determine the global optimal solution of atomic population;

**Step 5:** Update the speed and position of individual atoms according to the search strategy of hummingbirds;

**Step 6:** Determine whether the termination conditions of HOA are met. If yes, output the global

optimal network parameters; if no, continue to calculate the fitness function and update the element population distribution until the termination condition is met.

**Step 7:** Output the global optimal network parameters to obtain the optimal GRU network structure;

**Step 8:** Input the real-time aircraft trajectory characteristic parameters into the HOA-GRU maneuver trajectory prediction model, output the future aircraft trajectory characteristic parameters, and then obtain the future aircraft trajectory.

## 5. Simulation experiment and analysis

In order to verify the feasibility and effectiveness of the HOA-GRU prediction method in solving the problem of maneuver trajectory prediction, the number of GRU hidden units and the size of HOA atomic population were obtained by flight parameter training of aerial aircraft maneuver trajectory in this section. Then, two basic maneuvering cases and one complex maneuvering case were selected to test the effectiveness and robustness of the maneuver prediction model based on HOA-GRU. In order to verify the superiority of the proposed method, HOA-GRU is compared with RNN [15], LSTM [16], GRU [17] and HOA-LSTM, and the specific parameters of the compared algorithms are shown in Table 1. The simulation environment is including Windows 10, the CPU is 2.80 GHz, 8 GB memory, and the programming software is Matlab. Each simulation experiment was run 20 times, and the prediction results of 20 times were counted.

**Table 1.** Prediction algorithm parameter settings.

Algorithm	Parameter Settings
RNN	The number of hidden layer nodes is the same as that of HOA-GRU
LSTM	The number of hidden layer nodes is the same as that of HOA-GRU
GRU	The number of hidden layer nodes is the same as that of HOA-GRU
HOA-LSTM	The population size and number of hidden layer units are the same as HOA-GRU
HOA-GRU	The parameters are obtained by the following experimental analysis

### 5.1. Analysis and determination of HOA-GRU parameters

In order to determine the input step size  $n$  and output step size  $m$  of the aircraft maneuver prediction model, the performance of the prediction model under different input step size and output step size was analyzed.

Figure 3 shows the effects of different input step sizes and output step sizes on the performance of the HOA-GRU maneuvering prediction model. As can be seen from Figure 3(a), the Root Mean Square Error (RMSE) of aircraft maneuvering prediction based on the HOA-GRU does not change much as the input step size increases. As the output step size increases, the RMSE of HOA-GRU increases, but after the output step size is larger than 5, the RMSE changes little. As can be seen from Figure 3(b), the test prediction time slightly increases with the increase of input step size. With the increase of output step size, the prediction time does not change much. In summary, the input step size should be 2~5, and the output step size should be 1~3. In order to improve the prediction accuracy and real-time, this paper selects the input step size  $n = 5$  and the output step size  $m = 1$ .

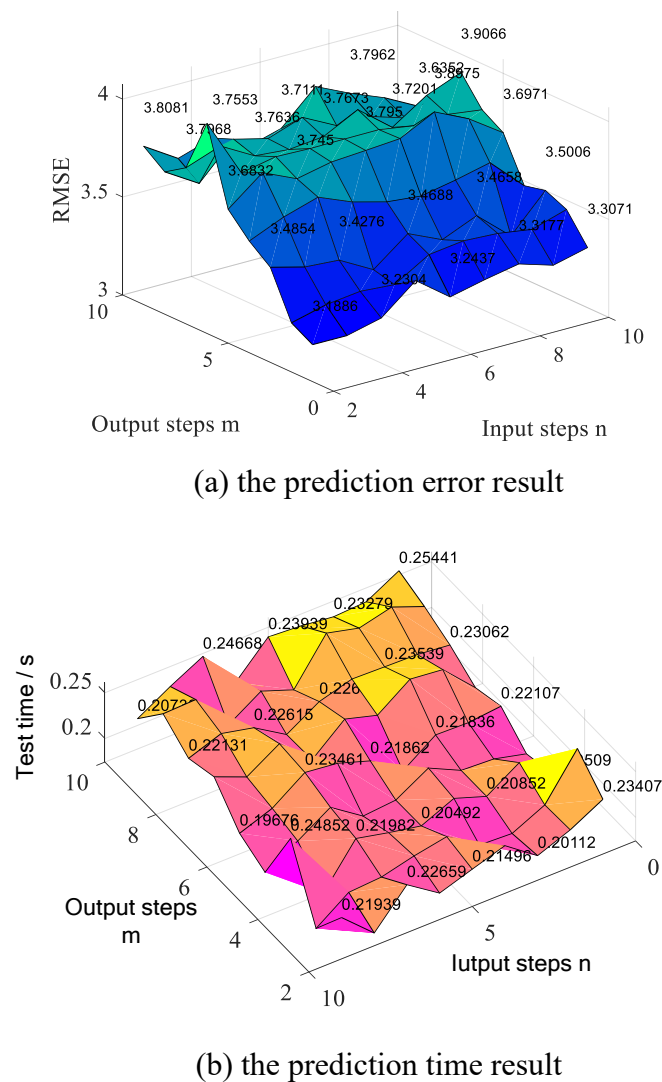
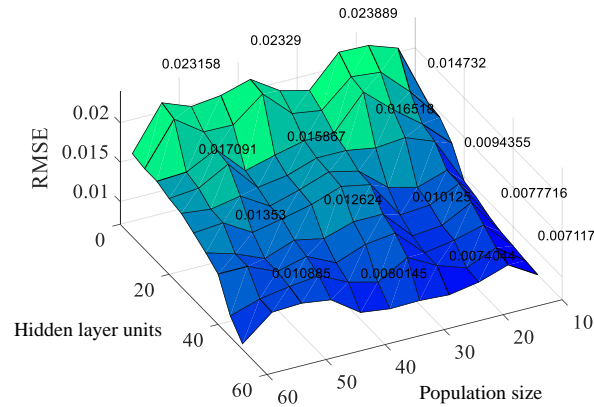


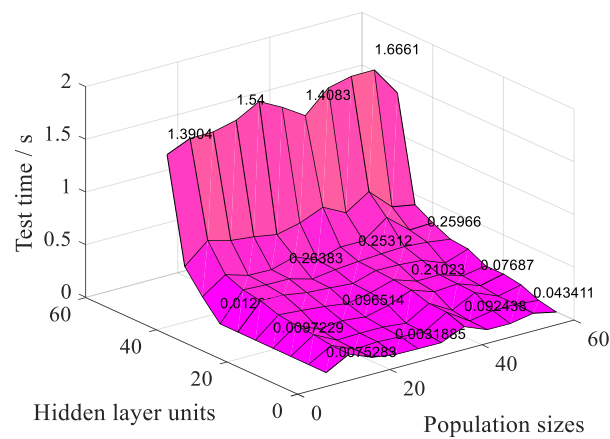
**Figure 3.** The impact of different input step and output step on the prediction performance of HOA-GRU.

In order to explore the effects of population size and number of hidden layer units on the performance of HOA-GRU based maneuver trajectory prediction model, the maneuver trajectory samples were used to test the prediction model, and the RMSE and prediction time under different parameters were calculated.

Figure 4 shows the effects of different population sizes and the number of hidden layer units on the performance of HOA-GRU-based maneuvering prediction model. As can be seen from Figure 4(a), with the increase of population atom number, RMSE has a slight increasing trend. As the number of hidden layer units increases, RMSE decreases. As can be seen from Figure 4(b), the prediction time changes little with the increase of population size. With the increase of the number of hidden layer units, the prediction time tends to increase, and after the number of hidden layer units reaches 40, the prediction time increases sharply. In summary, the population size is selected as 20, and the number of hidden layer units is set as 30.



(a) the prediction error result



(b) the prediction time result

**Figure 4.** The impact of different population size and number of hidden layer units on the prediction performance of HOA-GRU.

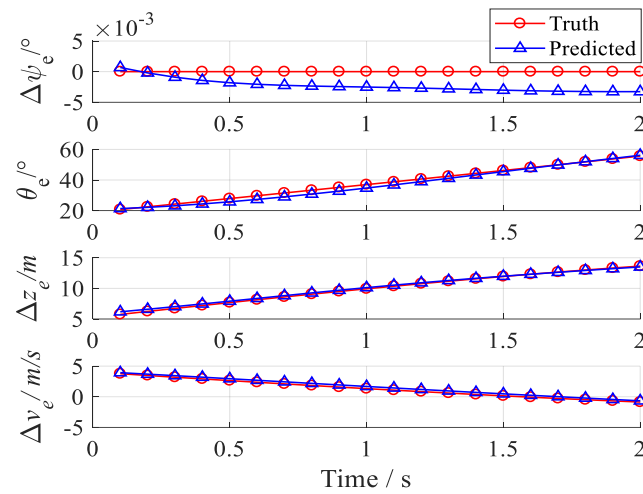
### 5.2. Simulation and analysis of maneuver trajectory prediction

According to the parameter analysis in the previous section, the HOA-GRU-based maneuver trajectory prediction model has an input step size of 5, an output step size of 1, a population size of 20, and a number of hidden layer elements of 30. In the simulation experiment of maneuver trajectory prediction in this section, three operating conditions are selected, including two basic maneuverings and one complex maneuvering. Meanwhile, the prediction performance statistics include RMSE and prediction time.

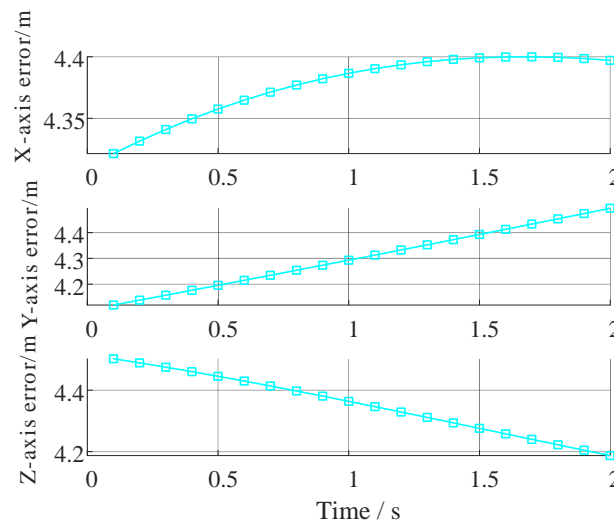
#### Case1: Climb maneuver

Figure 5 shows the result of climb maneuver prediction based on HOA-GRU algorithm. As can be seen from Figure 5(a), the error of the characteristic deviation angle change rate  $\Delta\psi_e$  of predicted trajectory based on HOA-GRU is less than  $0.005^\circ$ , the error of trajectory inclination angle  $\theta_e$  is less than  $1^\circ$ , the error of altitude change rate  $\Delta z_e$  is less than 0.05m, and the error of velocity change rate  $\Delta v_e$  is less than 0.2 m/s. As can be seen from Figure 5(b), the X-axis error, Y-axis error and Z-axis error of the position state of the climb maneuver trajectory do not exceed 4.4, 4.5 and 4.5 m respectively.

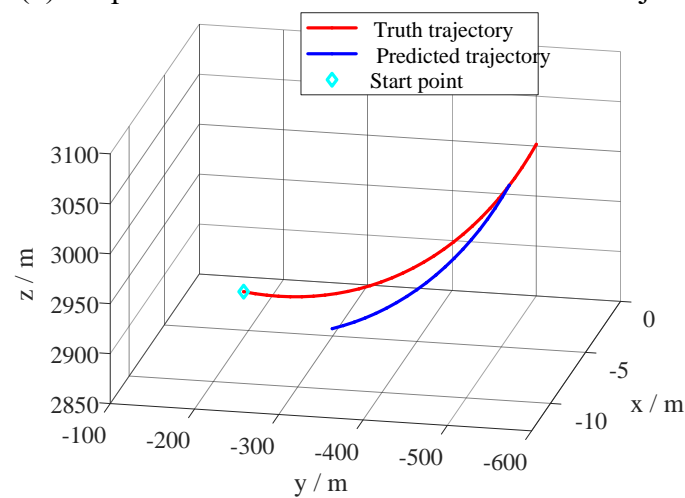
As can be seen from Figure 5(c), the climb maneuver trajectory based on HOA-GRU has little difference with the shape of the real trajectory.



(a) the prediction results of maneuver trajectory characteristics



(b) the position state error result of maneuver trajectory

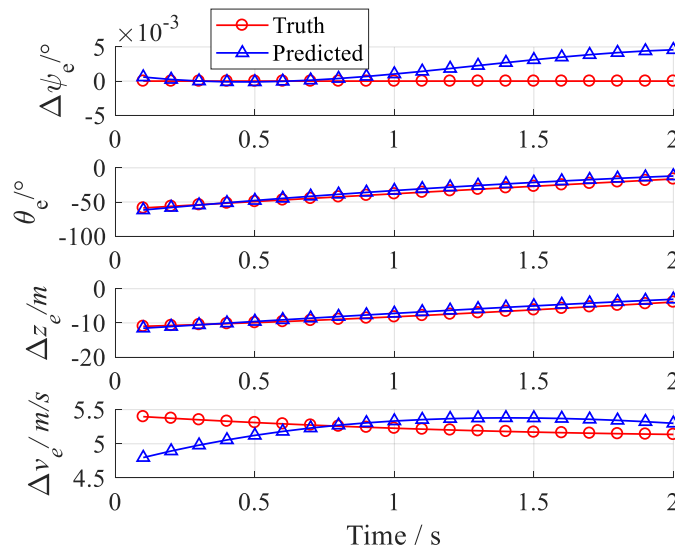


(c) the actual trajectory versus the predicted trajectory

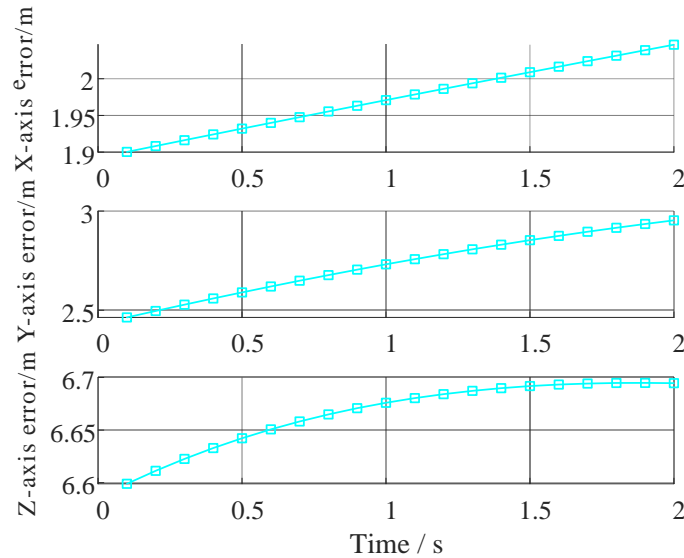
**Figure 5.** HOA-GRU prediction results for basic climb maneuver.

### Case2: Dive maneuver

Figure 6 shows the prediction results of dive maneuver based on HOA-GRU algorithm. As can be seen from Figure 6(a), the error of the characteristic deviation angle change rate  $\Delta\psi_e$  of the trajectory prediction based on HOA-GRU is less than  $0.005^\circ$ , the error of the track inclination angle  $\theta_e$  is less than  $2^\circ$ , the error of the altitude change rate  $\Delta z_e$  is less than 0.1m, and the error of the velocity change rate  $\Delta v_e$  is less than 0.5 m/s. As can be seen from Figure 6(b), the X-axis error of the position state of the subduction maneuver trajectory is less than 2.1 m, the Y-axis error is less than 3m, and the Z-axis error is less than 6.7 m. As can be seen from Figure 6(c), the maneuver trajectory based HOA-GRU has little difference with the shape of the real trajectory.

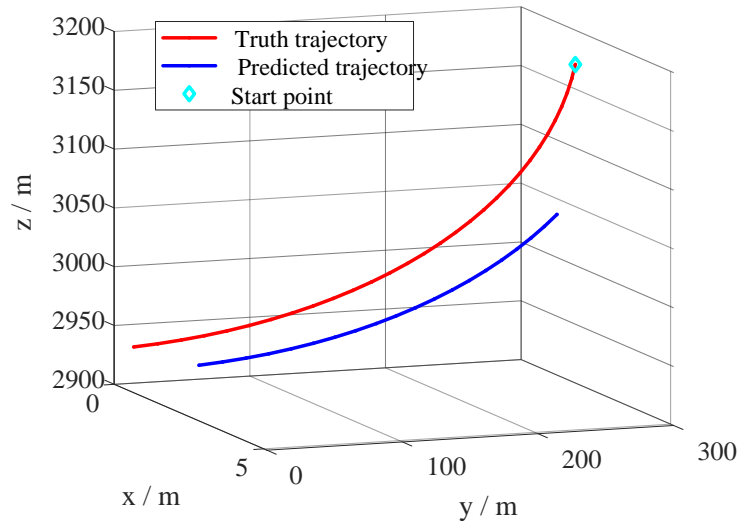


(a) the prediction results of maneuver trajectory characteristics



(b) the position state error result of maneuver trajectory

*Continued on next page*



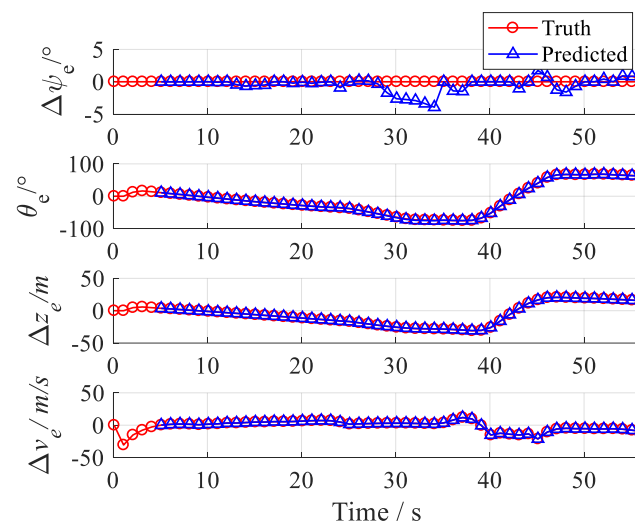
(c) the actual trajectory versus the predicted trajectory

**Figure 6.** HOA-GRU prediction results for basic dive maneuver.

### Case3: Complex maneuver

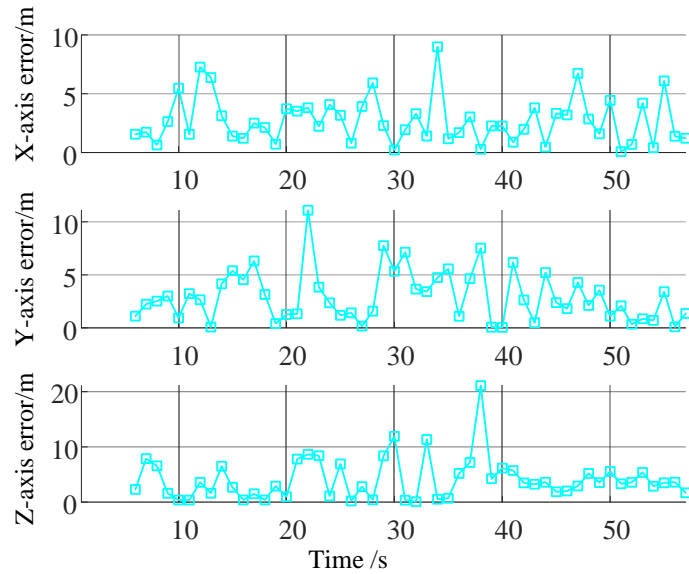
Figure 7 shows the prediction results of complex maneuvering based on HOA-GRU algorithm. As can be seen from Figure 7(a), the error of the characteristic deviation angle change rate  $\Delta\psi_e$ , the track inclination angle  $\theta_e$ , altitude change rate  $\Delta z_e$  and velocity change rate  $\Delta v_e$  of complex maneuver predicted trajectory are less than  $5^\circ$ ,  $5^\circ$ , 1 m and 1 m/s respectively. From Figure 7(b), the X-axis error, Y-axis error and Z-axis error of the position state of the complex maneuver trajectory are less than 15, 15 and 20 m respectively. As can be seen from Figure 7(c), the complex maneuver trajectory based on HOA-GRU almost matches the real trajectory.

In conclusion, the prediction error of aircraft maneuver trajectory based on HOA-GRU is small and meets the requirements of accuracy and time.

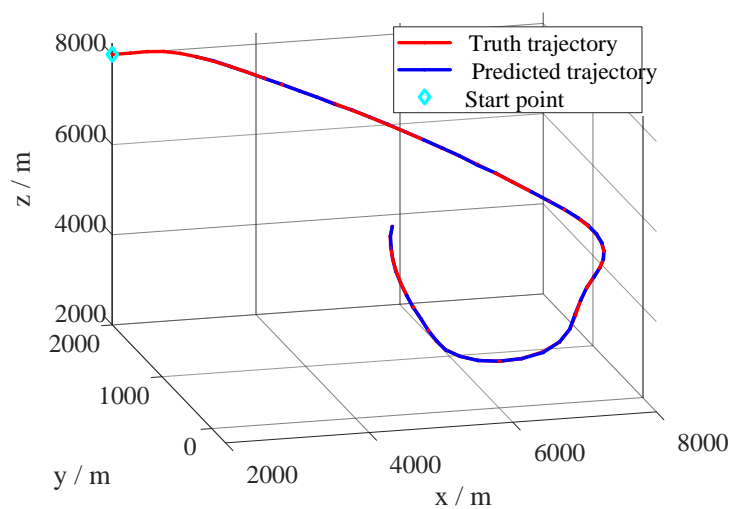


(a) the prediction results of maneuver trajectory characteristics

*Continued on next page*



(b) the position state error result of maneuver trajectory



(c) the actual trajectory versus the predicted trajectory

**Figure 7.** The prediction results for complex maneuver based on HOA-GRU.

Tables 2 and 3 respectively give the comparison results of the prediction error and prediction time of HOA-GRU and other prediction algorithms under three working conditions. As can be seen from Table 2, the prediction error of maneuver trajectory based on HOA-GRU is smaller than other algorithms, indicating that the prediction accuracy of this method is better than other algorithms.

**Table 2.** Comparison of prediction errors of HOA-GRU and other prediction algorithms.

No.	RNN	LSTM	GRU	HOA-LSTM	HOA-GRU
Case1	0.1179	0.1168	0.1151	0.1010	<b>0.0899</b>
Case2	0.0072	0.0076	0.0087	0.0049	<b>0.0045</b>
Case3	0.9757	0.2168	0.2453	0.0286	<b>0.0113</b>



As can be seen from Table 3, the prediction time of maneuver trajectory based on GRU is less than that of other algorithms, while the prediction time based on HOA-GRU is greater than that of GRU, but better than other algorithms.

**Table 3.** Comparison of prediction time of HOA-GRU and other prediction algorithms.

No.	RNN	LSTM	GRU	HOA-LSTM	HOA-GRU
Case1	0.0416 s	0.0066 s	<b>0.0023 s</b>	0.0029 s	0.0024 s
Case2	0.0098 s	0.0029 s	<b>0.0020 s</b>	0.0043 s	0.0021 s
Case3	1.9574 s	0.4662 s	<b>0.3550 s</b>	0.7567 s	0.3972 s

In conclusion, from the perspective of prediction accuracy, the prediction error of HOA-GRU is the smallest. From the perspective of prediction time, GRU has the shortest prediction time. Because HOA-GRU uses HOA optimization mechanism, the prediction time is more than GRU, but it is better than other algorithms, and meets the real-time requirements of air tasks.

## 6. Conclusions and discussion

In order to achieve fast and accurate maneuver trajectory prediction in air task, a practical data-driven algorithm of the maneuver trajectory prediction for the UAVs is proposed in this paper, which does not rely on accurate mathematical model and has global optimization performance. This method combines the advantages of model driven method and data-driven method, and obtains a better prediction accuracy and faster prediction speed for the UAVs.

Specifically, aiming at the problems of low accuracy and poor timing of aircraft maneuvering trajectory prediction, this prediction method uses the HOA to optimize the original GRU network. On the one hand, this method combines the advantages of GRU search strategy to overcome the problem of gradient disappearance in long time series prediction. On the other hand, it makes use of the advantages of HOA to avoid the gradient optimization of GRU falling into local optimization.

At present, the model is driven by real aircraft trajectory data under different working conditions, and many simulation results have been obtained. The results show that the proposed method can predict the trajectory of aircraft with a low error under the premise of real-time performance. Future studies should establish a more complete maneuvering trajectory unit library and increase the prediction accuracy and speed. Moreover, the multi-UAV cluster control experiments will be carried out to verify the effectiveness of maneuver trajectory prediction using the above algorithm in the real environment.

## Acknowledgments

The authors would like to thank the referees for their comments and suggestions which helped to improve the manuscript. This work was supported by the National Natural Science Foundation of China (61304036), and the China Postdoctoral Science Foundation (2014M562651, 2015T81132).

## Conflict of interest

The authors declare there is no conflict of interest.

## References

1. J. L. Yepes, I. Hwang, M. Rotea, New algorithms for aircraft intent inference and trajectory prediction, *J. Guid. Control Dyn.*, **30** (2012), 370–382. <https://doi.org/10.2514/1.26750>
2. L. Xie, Z. Wei, D. Ding, Z. Zhang, A. Tang, Long and short term maneuver trajectory prediction of UCAV based on deep learning, *IEEE Access*, **9** (2021), 32321–32340. <https://doi.org/10.1109/ACCESS.2021.3060783>
3. D. Ding, Z. Wei, S. Tang, Z. Huang, Robust maneuvering decision-making method for air combat using adaptive prediction weight, *Syst. Eng. Electron.*, **42** (2020), 2275–2284.
4. T. Wang, B. Huang, 4D flight trajectory prediction model based on improved Kalman filter, *J. Comput. Appl.*, **34** (2014), 1812–1815.
5. K. Zhang, J. Xiong, Fan. Li, T. Fu, Bayesian trajectory prediction for a hypersonic gliding reentry vehicle based on intent inference, *J. Astronaut.*, **39** (2018), 1258–1265. <https://doi.org/10.3873/j.issn.1000-1328.2018.11.008>
6. L. Wang, Q. Xing, Y. Mao, A track forecasting algorithm of boost-glide unpropulsive skipping vehicle, *J. Air Force Eng. Univ. (Nat. Sci. Ed.)*, **16** (2015), 24–27.
7. Q. Wang, Z. Zhang, Z. Wang, Y. Wang, W. Zhou, The trajectory prediction of spacecraft by grey method, *Meas. Sci. Technol.*, **27** (2016), 085011–085020. <https://doi.org/10.1088/0957-0233/27/8/085011>
8. C. G. Prevost, A. Desbiens, E. Gagnon, Extended kalman filter for state estimation and trajectory prediction of a moving object detected by an unmanned aerial vehicle, in *2007 American Control Conference*, (2007), 1805–1810. <https://doi.org/10.1109/ACC.2007.4282823>
9. G. Li, H. Zhang, G. Tang, Typical trajectory characteristics of hypersonic glide vehicle, *J. Astronaut.*, **36** (2015) 397–403. <https://doi.org/10.3873/j.issn.1000-1328.2015.04.005>
10. C. Han, J. Xiong, K. Zhang, X. Lan, Decomposition ensemble trajectory prediction algorithm for hypersonic vehicle, *Syst. Eng. Electron.*, **40** (2018), 151–158. <https://doi.org/10.3969/j.issn.1001-506X.2018.01.22>
11. M. Q. Chen, Aircraft climb trajectory prediction using neural network, *Appl. Mech. Mater.*, **373-375** (2013), 1247–1250. <https://doi.org/10.4028/www.scientific.net/AMM.373-375.1247>
12. X. Wang, R. Yang, J. Zuo, X. Xu, L. Yue, Trajectory prediction of target aircraft based on HPSO-TPFENN neural network, *J. Northwest. Polytech. Univ.*, **37** (2019), 612–620. <https://doi.org/10.1051/jnwpu/20193730612>
13. H. Zhang, C. Huang, S. Tang, Y. Xuan, CNN-based real-time prediction method of flight trajectory of unmanned combat aerial vehicle, *Acta Armamentarii*, **41** (2020), 1894–1903. <https://doi.org/10.3969/j.issn.1000-1093.2020.09.022>
14. Y. Lecun, Y. Bengio, G. Hinton, Deep learning, *Nature*, **521** (2015), 436–444. <https://doi.org/10.1038/nature14539>
15. S. L. Churchill, RNN composition of thematically diverse video game melodies, *Comput. Games*, **8** (2019), 41–58. <https://doi.org/10.1007/s40869-018-0063-x>
16. S. Hochreiter, J. Schmidhuber, Long short-term memory, *Neural Comput.*, **9** (1997), 1735–1780. <https://doi.org/10.1162/neco.1997.9.8.1735>
17. F. Rui, Z. Zuo, L. Li, Using LSTM and GRU neural network methods for traffic flow prediction, in *2016 31st Youth Academic Annual Conference of Chinese Association of Automation (YAC)*, (2016), 324–328. <https://doi.org/10.1109/YAC.2016.7804912>

18. Z. Zhang, C. Huang, D. Ding, S. Tang, B. Han, H. Huang, Hummingbirds optimization algorithm-based particle filter for maneuvering target tracking, *Nonlinear Dyn.*, **97** (2019), 1227–1243. <https://doi.org/10.1007/s11071-019-05043-0>
19. Z. Zhang, C. Huang, H. Huang, S. Tang, K. Dong, An optimization method: hummingbirds optimization algorithm, *J. Syst. Eng. Electron.*, **29** (2018), 386–404. <https://doi.org/10.21629/JSEE.2018.02.19>
20. J. Y. Yoon, A. H. Lee, H. J. Lee, Rendezvous: opportunistic data delivery to mobile users by UAVs through target trajectory prediction, *IEEE Trans. Veh. Technol.*, **69** (2020), 2230–2245. <https://doi.org/10.1109/TVT.2019.2962391>
21. B. Hu, H. Yang, L. Wang, S. Chen, A trajectory prediction based intelligent handover control method in UAV cellular networks, *China Commun.*, **16** (2019), 1–14. Available from: <https://ieeexplore.ieee.org/document/8633299>.



AIMS Press

©2022 the Author(s), licensee AIMS Press. This is an open access article distributed under the terms of the Creative Commons Attribution License (<http://creativecommons.org/licenses/by/4.0>)